# Chaotic Motion of a Solid through Ideal Fluid

Hassan Aref and Scott W. Jones
*Department of Theoretical and Applied Mechanics*
*University of Illinois at Urbana-Champaign*
*Urbana, IL 61801-2935, USA*

(Submitted to *Phys. Fluids A* as a Letter on June 7, 1993)

Numerical evidence is presented that the motion of a solid body through incompressible, inviscid fluid, moving irrotationally and otherwise at rest, is chaotic. Chaos manifests itself both in the orientation of the body relative to fixed directions in space, and in the trajectory of a definite point in the body when referred to a fixed frame of reference.

PACS: 47.20.Tg; 47.15.Hg

The motion of a solid body through incompressible, inviscid, irrotational fluid otherwise at rest is a classical problem in hydrodynamics and aerodynamics of great significance. It was shown by Kirchhoff[1,2] more than a century ago that the problem reduces to a set of *ordinary* differential equations which generalize Euler's equations[3] describing the motion of a solid body in a vacuum. The Kirchhoff equations present a most remarkable simplification of a problem that in principle involves an infinite number of degrees of freedom. Surprisingly, the literature exploring these equations from the point of view of dynamical systems theory is rather sparse.

In a significant paper Kozlov & Oniscenko[4] achieved a characterization of the integrable cases of Kirchhoff's equations. They suggest that when the conditions of their main theorem are not met, the motion of the body will be chaotic. Neither the exact nature of this chaotic motion, nor evidence for its existence, appear to have been given. It is the purpose of this Letter to provide numerical evidence that the Kirchhoff equations do, indeed, have chaotic solutions and to take a first step in providing a physical description of such motions. We shall see, in particular, that chaos manifests itself both in the orientation dynamics of the body and in the geometry of its trajectory in space.

Since the solutions of the potential flow problem about a body represent the "outer" solution of the "full" flow problem (i.e., the problem in the presence of viscosity), we believe that the distinction between regular and chaotic motion is of importance for such fundamental aspects of the flow about bodies as separation and for the nature of the pressure distribution over the bounding surface of the body. On the basis of this argument we expect to see vestiges of the chaotic motion found for the idealized problem of inviscid potential flow in the full viscous flow problem.

An important step is to cast Kirchhoff's equations in the familiar language of Hamiltonian dynamics. This is, in essence, achieved in §122 of Lamb's classic treatise[5], but it is unlikely that a modern reader would immediately make the connection. We present some of the details here. A more complete version will appear elsewhere.

The equations of motion as written by Kirchhoff[1,2] were in terms of the vectors of velocity, $\mathbf{U}$, and angular velocity, $\Omega$, of the body referred instantaneously to a frame of coordinates moving with the body:

$$\frac{d}{dt}\left(\frac{\partial T_{tot}}{\partial \mathbf{U}}\right) + \boldsymbol{\Omega} \times \frac{\partial T_{tot}}{\partial \mathbf{U}} = \mathbf{0}, \tag{1}$$

$$\frac{d}{dt}\left(\frac{\partial T_{tot}}{\partial \boldsymbol{\Omega}}\right) + \boldsymbol{\Omega} \times \frac{\partial T_{tot}}{\partial \boldsymbol{\Omega}} + \mathbf{U} \times \frac{\partial T_{tot}}{\partial \mathbf{U}} = \mathbf{0}. \tag{2}$$

Here $T_{tot}$ is the kinetic energy of the solid body *and* the surrounding fluid:

$$T_{tot} = \tfrac{1}{2}\,\mathbf{U} \cdot (\mathbf{T} + m\mathbf{1})\mathbf{U} + \tfrac{1}{2}\,\boldsymbol{\Omega} \cdot (\mathbf{J} + \mathbf{I})\boldsymbol{\Omega} + \mathbf{U} \cdot \mathbf{S}\boldsymbol{\Omega}, \tag{3}$$

where m is the mass and $\mathbf{I}$ is the inertia tensor of the solid body, $\mathbf{1}$ is the unit $3 \times 3$ identity tensor, and $\mathbf{T}$, $\mathbf{S}$ and $\mathbf{J}$ make up the $6 \times 6$ *added mass tensor*, $T_{\alpha\beta}$, as follows[5,6]:

$$\{T_{\alpha\beta}\} = \begin{Bmatrix} \mathbf{T} & \mathbf{S} \\ \mathbf{S}^T & \mathbf{J} \end{Bmatrix}, \tag{4}$$

with $\mathbf{S}^T$ the transpose of $\mathbf{S}$. The elements of $\mathbf{T}$, $\mathbf{S}$, and $\mathbf{J}$ depend only on the body shape[5,6]. For certain simple body shapes, such as ellipsoids, these constants are known analytically. In writing (3) a common assumption of rigid body dynamics, that the origin of the moving coordinate system coincides with the center of mass of the body, has been made.

We may write these equations of motion more explicitly as follows: From (3) we introduce a generalized momentum (the *linear impulse*[5])

$$\mathbf{P} = \left(\frac{\partial T_{tot}}{\partial \mathbf{U}}\right)_{\boldsymbol{\Omega}} = (\mathbf{T} + m\mathbf{1})\mathbf{U} + \mathbf{S}\boldsymbol{\Omega}, \tag{5}$$

and a generalized angular momentum (the *angular impulse*[5])

$$\mathbf{L} = \left(\frac{\partial T_{tot}}{\partial \boldsymbol{\Omega}}\right)_{\mathbf{U}} = (\mathbf{J} + \mathbf{I})\boldsymbol{\Omega} + \mathbf{S}^T\mathbf{U}\,. \tag{6}$$

Equations (1), (2) then take the form

$$\dot{\mathbf{P}} + \boldsymbol{\Omega} \times \mathbf{P} = \mathbf{0}, \tag{7}$$

and

$$\dot{\mathbf{L}} + \boldsymbol{\Omega} \times \mathbf{L} + \mathbf{U} \times \mathbf{P} = \mathbf{0}. \tag{8}$$

It is immediately seen from (7) and (8) that the quantities $\mathbf{P}\cdot\mathbf{P}$ and $\mathbf{L}\cdot\mathbf{P}$ are integrals of the motion. We note for later reference that

$$2T_{tot} = \mathbf{U} \bullet \mathbf{P} + \Omega \bullet \mathbf{L}. \tag{9}$$

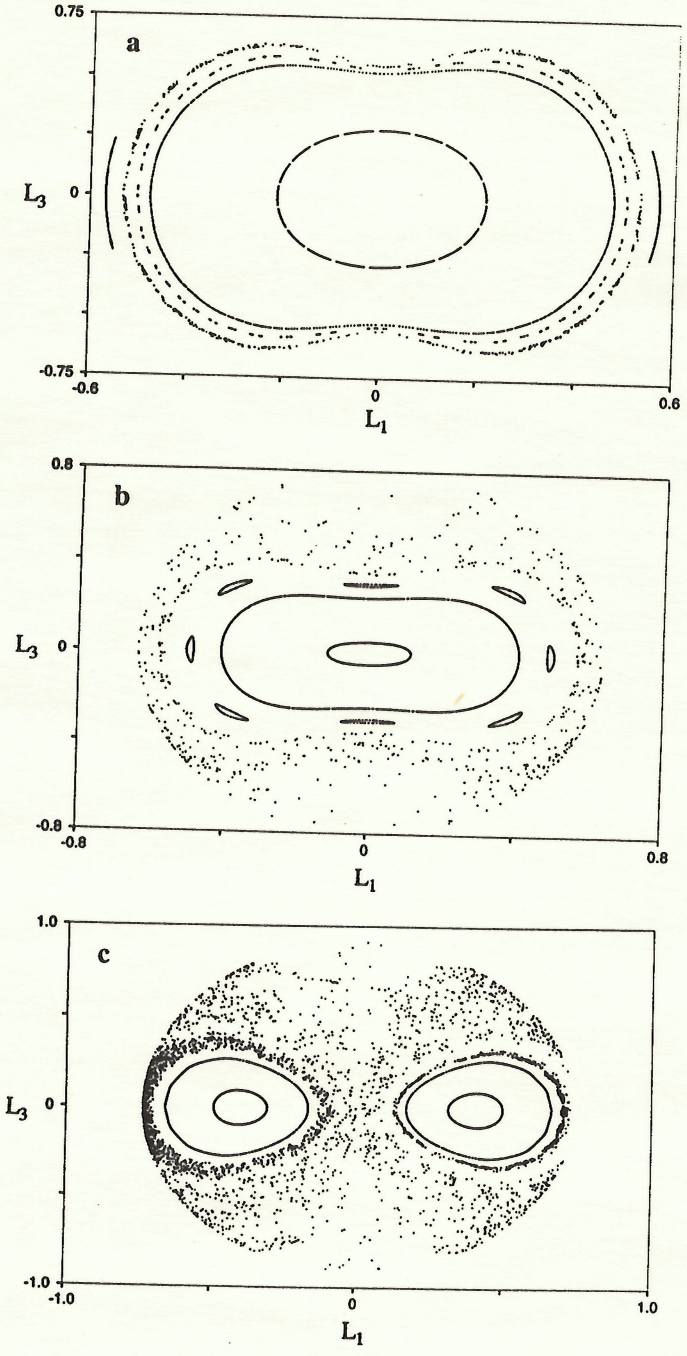


Figure 1: Poincaré sections ($L_x$, $L_z$) for $P_z = 0$ with $\mathbf{L} \bullet \mathbf{P} = 0$.
Several initial conditions are shown in each panel and (a) $\delta = 0.5$; (b) 1.0; (c) 2.0.

We adopt the point of view that the "generalized coordinates" of this system are the three components of $\mathbf{R}$ and the nine elements, $A_{ij}$, of the orthogonal matrix $\mathbf{A}$ that determines the orientation of the body-fixed coordinate frame relative to a fixed, inertial, "laboratory" frame. The orthogonality relations for $\mathbf{A}$ are then viewed as integrals of the motion of this system. Equations (7)-(8) constitute a system of six coupled ODEs for the components of $\mathbf{U}$ and $\Omega$. In order to obtain the actual motion of the solid body relative to the "laboratory" frame, one must supplement these equations by additional ODEs for the position of the origin of the body-fixed system, $\mathbf{R}$, and for its orientation. These equations are

$$\dot{\mathbf{R}} = \mathbf{A}\mathbf{U}, \tag{10}$$

$$\dot{A}_{ij} = -\varepsilon_{jkl}\, A_{il}\, \Omega_k. \tag{11}$$

where $\dot{\mathbf{R}}$, $\dot{A}_{ij}$ are the time derivatives of $\mathbf{R}$ and $A_{ij}$, respectively, and $\varepsilon_{jkl}$ is the completely antisymmetric tensor of rank three.

Kirchhoff's equations (1)-(2) are the Lagrangian equations of motion. The Lagrangian is $T_{tot}$. We may transform to Hamilton's canonical equations by considering the Legendre transform

$$H = T_{tot} - \dot{\mathbf{R}} \bullet \frac{\partial T_{tot}}{\partial \dot{\mathbf{R}}} - \dot{A}_{ij}\, \frac{\partial T_{tot}}{\partial \dot{A}_{ij}} = T_{tot} - \mathbf{U} \bullet \frac{\partial T_{tot}}{\partial \mathbf{U}} - \Omega \bullet \frac{\partial T_{tot}}{\partial \boldsymbol{\Omega}}. \tag{12}$$

Hence, by (9)

$$H = T_{tot} - \mathbf{U} \bullet \mathbf{P} - \Omega \bullet \mathbf{L} = -\, T_{tot}. \tag{12}$$

Since

$$dT_{tot} = \mathbf{P} \bullet d\mathbf{U} + \mathbf{L} \bullet d\Omega, \tag{13}$$

we now have as complements to the definitions (5), (6):

$$\mathbf{U} = -\left(\frac{\partial H}{\partial \mathbf{P}}\right)_{\mathbf{L}} = \left(\frac{\partial T_{tot}}{\partial \mathbf{P}}\right)_{\mathbf{L}} \quad ; \quad \Omega = -\left(\frac{\partial H}{\partial \mathbf{L}}\right)_{\mathbf{P}} = \left(\frac{\partial T_{tot}}{\partial \mathbf{L}}\right)_{\mathbf{P}}. \tag{14}$$

Combining these results with (7)-(8) we easily see that H itself is an integral of the motion.

The generalized coordinates being the components of $\mathbf{R}$ and the $A_{ij}$, we introduce generalized momenta conjugate to these by

$$\Pi_i = \frac{\partial T_{tot}}{\partial \dot{R}_i} = A_{ik}\, P_k \;\; ; \;\; B_{ij} = \frac{\partial T_{tot}}{\partial \dot{A}_{ij}} = \tfrac{1}{2}\, A_{im}\, \varepsilon_{jmk}\, L_k. \tag{15}$$

The appropriate Poisson-Lie bracket for quantities $f$, g that do not depend on $\mathbf{R}$ is

$$\{f,g\} = \frac{\partial f}{\partial A_{ij}} \frac{\partial g}{\partial B_{ij}} - \frac{\partial f}{\partial B_{ij}} \frac{\partial g}{\partial A_{ij}} . \tag{16}$$

A somewhat tedious derivation using (15) then gives:

$$\{f,g\} = \mathbf{L} \cdot \frac{\partial g}{\partial \mathbf{L}} \times \frac{\partial f}{\partial \mathbf{L}} + \mathbf{P} \cdot \left(\frac{\partial g}{\partial \mathbf{L}} \times \frac{\partial f}{\partial \mathbf{P}} - \frac{\partial f}{\partial \mathbf{L}} \times \frac{\partial g}{\partial \mathbf{P}}\right). \tag{17}$$

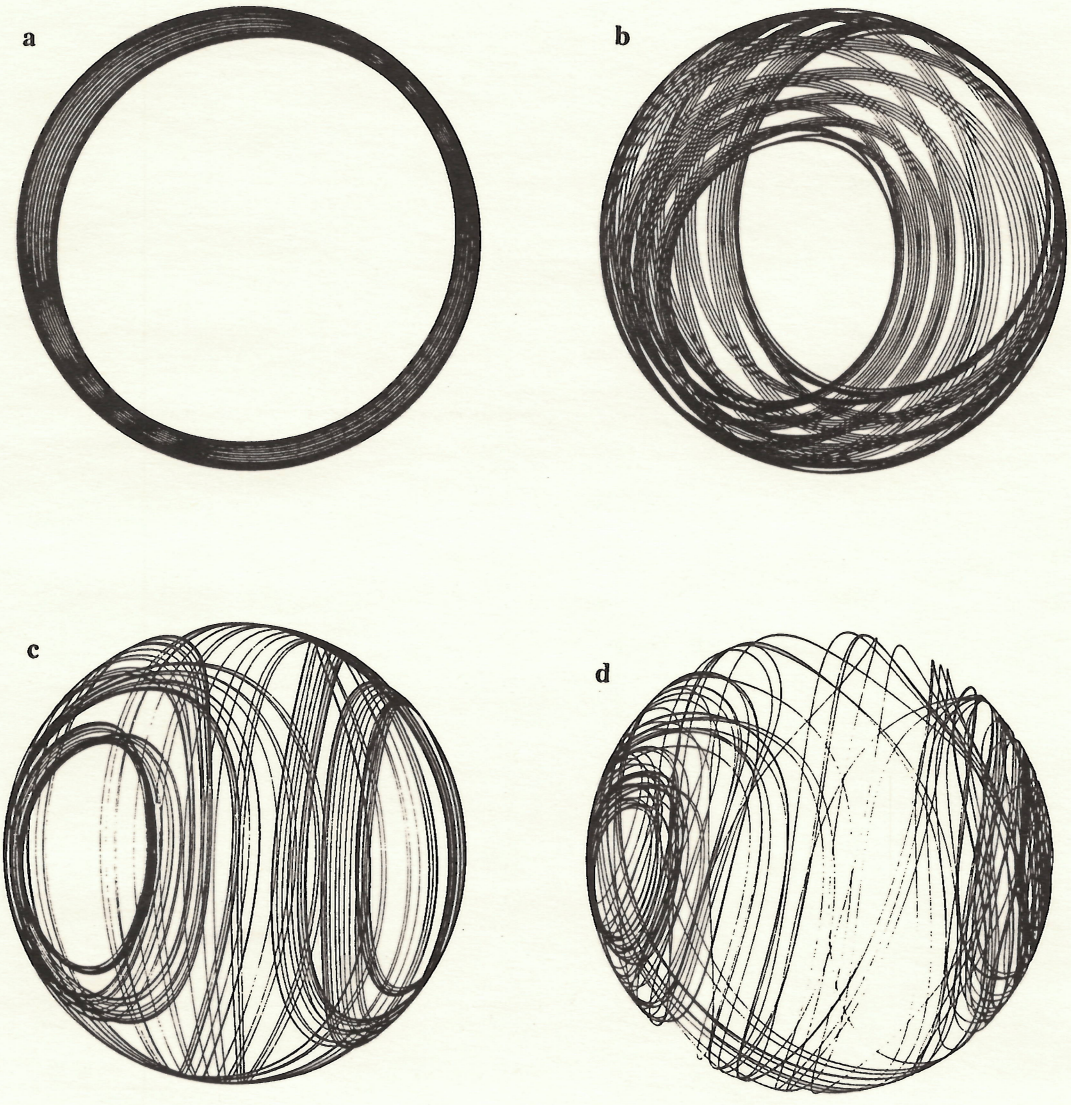


Figure 2: Illustrations of the variation of body orientation for the four initial conditions in Fig.1(b). The trajectories shown would be traced out by the tip of a "pointer", rigidly attached to the body, on a sphere that followed the motion of the body centroid but did not rotate relative to the laboratory frame.

In particular, we see from (14) that

$$\{H,f\} = -\frac{\partial f}{\partial \mathbf{L}} \bullet (\Omega \times \mathbf{L} + \mathbf{U} \times \mathbf{P}) - \frac{\partial f}{\partial \mathbf{P}} \bullet \Omega \times \mathbf{P}. \tag{18}$$

Thus, we finally obtain the equations of motion (7), (8) in the desired form

$$\dot{\mathbf{P}} = \{H,\mathbf{P}\} \quad ; \quad \dot{\mathbf{L}} = \{H,\mathbf{L}\}. \tag{20}$$

This is the Hamiltonian formulation. Lamb[5] uses the notation T` for our H, but the treatment is less transparent and the connection to Hamiltonian mechanics and a Poisson-Lie bracket is not made explicitly.

We note the "elementary" brackets

$$\{P_i,P_j\} = 0 \; ; \; \{L_i,L_j\} = -\varepsilon_{ijk} L_k \; ; \; \{P_i,L_j\} = -\varepsilon_{ijk} P_k. \tag{21}$$

It follows from these that any function of $\mathbf{P}$ and $\mathbf{L}$ commutes with both $\mathbf{P}^2$ and $\mathbf{L}\bullet\mathbf{P}$. In particular, the two integrals $\mathbf{P}^2$ and $\mathbf{L}\bullet\mathbf{P}$ are in involution. The dynamics of Kirchhoff's equations can therefore be reduced to the subspace of the six-dimensional $(\mathbf{P},\mathbf{L})$-space given by $|\mathbf{P}| = \text{const.}$, and $\mathbf{L}\bullet\mathbf{P} = \text{const}$. Along with the constancy of the total kinetic energy, this reduces the problem to motion on a three-dimensional manifold. This formulation is used as a basis for numerical exploration of the system and identification of integrable and chaotic solutions.

We have integrated the equations (7), (8), (10), (11) numerically for various body shapes and a number of initial conditions. We chose an ellipsoid with semi-axes (a,b,c) = (1, 0.8, 0.6), which does not satisfy the integrability condition of Kozlov & Oniscenko[4]. For all motions considered we chose $\mathbf{L}\bullet\mathbf{P} = 0$. A Poincaré section is obtained by recording points $(L_x, L_z)$ for which $P_z = 0$. Three examples of such sections are shown in Figure 1. The three sections correspond to three different values of the density ratio of the solid body (assumed homogeneous) to the fluid, $\delta \equiv \rho_{fluid}/\rho_{solid}$. This parameter determines the relative importance of fluid to solid inertia. If $\delta << 1$, we expect the problem to approach the integrable Euler equations for a body in a vacuum. On the other hand, for $\delta >> 1$ the problem approaches that of a very light but rigid "bubble" moving through the fluid. In Figure 1 we have (a) $\delta$=0.5; (b) 1.0; (c) 2.0. The increasing amount of apparent chaos in these sections corresponds with physical intuition.

Now, consider Figure 1(b) in more detail. Section points for four different initial conditions are plotted. The two innermost elliptical curves correspond to two initial conditions that yielded regular motion. There follows a period-8 "island chain." Finally, the last initial condition used produced the chaotic splatter of points at the outer bound of the plot. Figure 2 provides a different view of these four motions. In all four panels of Figure 2 we show the curve traced out by a "pointer," rigidly attached to the ellipsoid, on a sphere centered at the centroid of the ellipsoid and following along in its motion but *without* rotating relative to the laboratory frame. Hence, each panel in Figure 2 gives a representation of the *change in orientation* of the solid ellipsoid as it moves through the fluid. Panels (a) and (b) of Figure 2 correspond to the two regular motions seen in the section of Figure 1(b). Panel (d) corresponds to the chaotic trajectory in Figure 1(b). The period-8 island chain in Figure 1(b) leads to panel (c) of Figure 2, and one can almost pick out the period-8 motion in Figure 2(c) as well. Taken together Figure 1 and 2 provide numerical evidence for the existence of chaotic motions of the solid body, and show that one can observe this chaotic motion

through the changes in orientation of the body as a function of time.

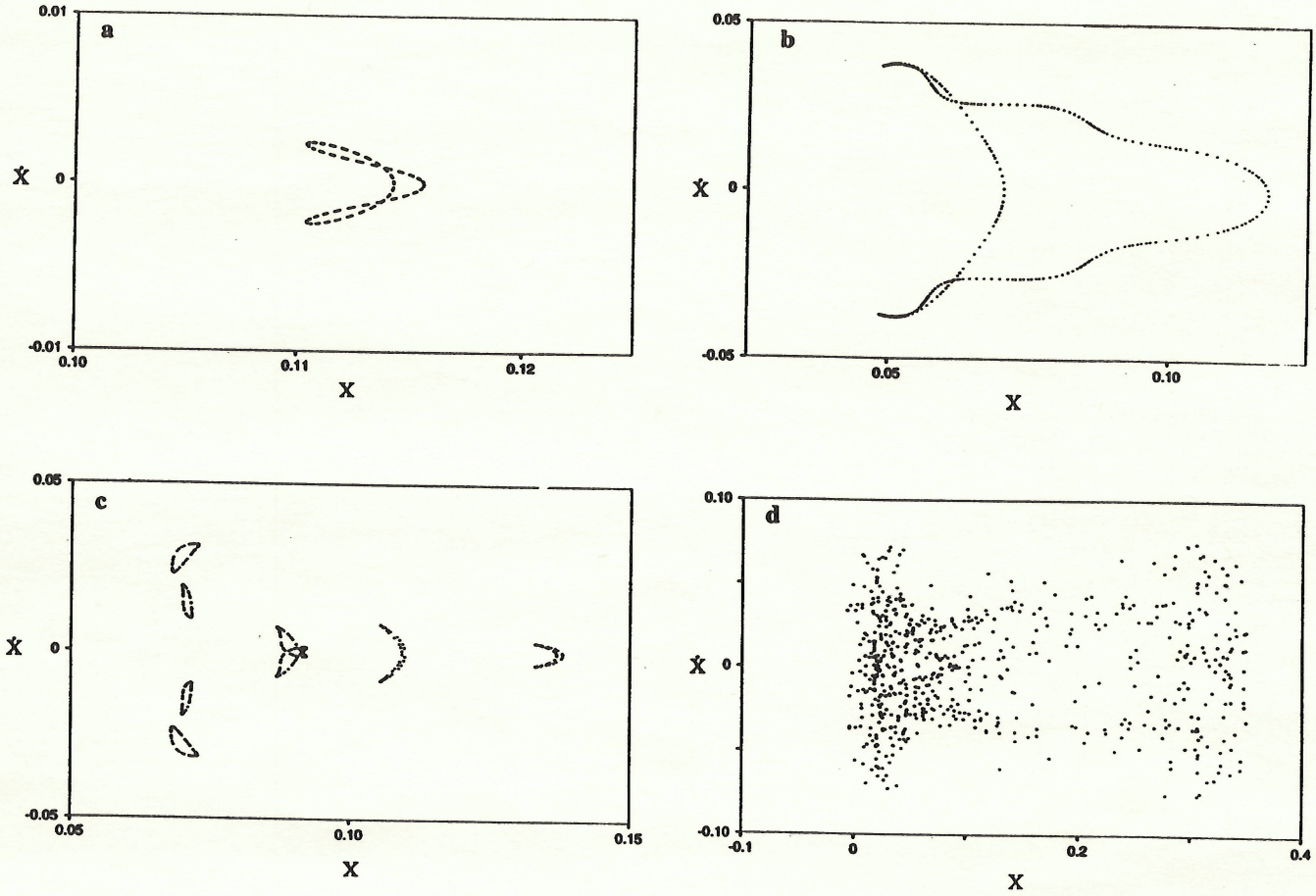


Figure 3: (X,Ẋ) Poincaré sections of the trajectory of the centroid of the body for the four initial conditions shown in Figure 1(b). The period-8 section in panel (c) corresponds to the period-8 island chain in Figure 1(b).

Due to the close coupling of orientation dynamics and the actual trajectory in space of the body – see Eqs.(10)-(11) in particular – one would expect to also be able to detect the progression from regular to chaotic motion seen in Figure 1(b) in a suitable plot of the trajectory of the body centroid. This is indeed the case as Figure 3 illustrates. For each of the four initial conditions discussed in relation to Figure 1(b) and Figure 2 we have plotted an $(X, \dot{X})$ Poincaré section in Figure 3. The times at which an $(X, \dot{X})$ point is plotted in Figure 3 correspond to the section points in Figure 1(b). However, in order to obtain the best perspective we have rotated the laboratory frame for each panel of Figure 3 such that the plane in which $(X, \dot{X})$ is measured is perpendicular to the initial value of the impulse. The $(X, \dot{X})$-plane is thus fixed for each panel, but is not the same from panel to panel since the different initial conditions have different initial impulse vectors. For this reason it would not make sense to superimpose panels (a)-(d) of Figure 3. Once again, the progression from regular motion to chaos is clearly seen, and the period-8 structure in Figure 3(c) matches the corresponding structure discussed in conjunction with Figure 1(b) and 2(c). Numerous similar plots have been generated for other choices of the parameters.

In summary, we have presented compelling and consistent numerical evidence that Kirchhoff's equations are in general non-integrable, and that chaotic motion of a solid body moving through a fluid can be detected either by monitoring changes in orientation of the body (regardless of displacement) or by monitoring the trajectory in space of a fixed point in the body (regardless of orientation). In the cases presented here chaos is observable in both these measures at once. Several additional questions present themselves: Can chaotic body motion be detected by monitoring the pressure field on the body? When will the trajectory of a passively advected particle in the flow induced by the motion of the body be chaotic? Will the time series produced by the Eulerian velocity field at a point display chaos when the "Lagrangian" motion of the body is chaotic? And so on. The correspondence between chaotic motion of the body and chaos in other diagnostics of the flow is not *a priori* obvious, and is currently being explored.

The results presented here were first reported by one of us (SWJ) at the Midwestern Universities Fluid Mechanics retreat, April 1-3, 1993.

We are indebted to D. D. Holm for discussions, for alerting us to Ref.4, and for communicating to us prior to publication results obtained jointly with R. Camassa on certain integrable cases of Kirchhoff's equations. This research was supported by University of Illinois.

## REFERENCES

1. Kirchhoff, G. 1882 "Über die Bewegung eines Rotationskörpers in einer Flüssigkeit." In *Collected Works,* J. A. Barth, Leipzig, pp. 376-403.
2. Kirchhoff, G. 1897 *Mechanik,* ed. B. G. Teubner, Leipzig. Ch. 19, pp.232-250.
3. Whittaker, E. T. 1937 *A Treatise on the Analytical Mechanics of Particles and Rigid Bodies.* Fourth edition. Cambridge University Press.
4. Kozlov, V. V. & Oniscenko, D. A. 1982 "Nonintegrability of Kirchhoff's equations." *Sov. Math. Dokl.* **26**, 495-498.
5. Lamb, H. 1932 *Hydrodynamics.* Sixth edition. Cambridge University Press, Ch. VI.
6. Milne-Thomson, L. M. 1968 *Theoretical Hydrodynamics.* Macmillan, London. Ch. XVII.

# List of Recent TAM Reports

| No. | Authors | Title | Date |
|---|---|---|---|
| 495 | Stewart, D. S., and B. W. Asay | Discrete modeling of beds of propellant exposed to strong stimulus | Apr. 1991 |
| 496 | Klein, R., and D. S. Stewart | The relation between curvature, rate state dependence, and detonation velocity | Apr. 1991 |
| 497 | Powers, J. M., and D. S. Stewart | Approximate solutions for oblique detonations in the hypersonic limit | Apr. 1991 |
| 498 | Davidson, M. T., K. L. Kuster, K. W. Quinn, N. A. Sluz, and G. Stojkovich | Twenty-fifth student symposium on engineering mechanics, M. E. Clark, coord. (1988) | Feb. 1992 |
| 499 | Cardenas, H. E., W. C. Crone, D. J. Scott, G. G. Stewart, and B. F. Tatting | Twenty-sixth student symposium on engineering mechanics, M. E. Clark, coord. (1989) | Mar. 1992 |
| 700 | Juister, C. E., D. W. Newport, C. S. Payne, J. M. Peters, M. P. Thomas, and J. C. Trovillion | Twenty-seventh student symposium on engineering mechanics, M. E. Clark, coord. (1990) | Apr. 1992 |
| 701 | Bernard, R. T., D. W. Claxon, J. A. Jones, V. R. Nitzsche, and M. T. Stadtherr | Twenty-eighth student symposium on engineering mechanics, M. E. Clark, coord. (1991) | Apr. 1992 |
| 702 | Greening, L. E., P. J. Joyce, S. G. Martensen, M. D. Morley, J. M. Ockers, M. D. Taylor, and P. J. Walsh | Twenty-ninth student symposium on engineering mechanics, J. W. Phillips, coord. (1992) | May 1992 |
| 703 | Kuah, H. T., and D. N. Riahi | Instabilities and transition to chaos in plane wakes | Nov. 1992 |
| 704 | Stewart, D. S., K. Prasad, and B. W. Asay | Simplified modeling of transition to detonation in porous energetic materials | Nov. 1992 |
| 705 | Stewart, D. S., and J. B. Bdzil | Asymptotics and multi-scale simulation in a numerical combustion laboratory | Jan. 1993 |
| 706 | Hsia, K. J., Y.-B. Xin, and L. Lin | Numerical simulation of semi-crystalline Nylon 6: Elastic constants of crystalline and amorphous parts | Jan. 1993 |
| 707 | Hsia, K. J., and J. Q. Huang | Curvature effects on compressive failure strength of long fiber composite laminates | Jan. 1993 |
| 708 | Jog, C. S., R. B. Haber, and M. P. Bendsoe | Topology design with optimized, self-adaptive materials | Mar. 1993 |
| 709 | Barkey, M. E., D. F. Socie, and K. J. Hsia | A yield surface approach to the estimation of notch strains for proportional and nonproportional cyclic loading | Apr. 1993 |
| 710 | Feldsien, T. M., A. D. Friend, G. S. Gehner, T. D. McCoy, K. V. Remmert, D. L. Riedl, P. L. Scheiberle, and J. W. Wu | Thirtieth student symposium on engineering mechanics, J. W. Phillips, coord. (1993) | Apr. 1993 |
| 711 | Weaver, R. L. | Anderson localization in the time domain: Numerical studies of waves in two-dimensional disordered media | Apr. 1993 |
| 712 | Cherukuri, H. P., and T. G. Shawki | An energy-based localization theory: Part I—Basic framework | Apr. 1993 |
| 713 | Manring, N. D., and R. E. Johnson | Modeling a variable-displacement pump | June 1993 |
| 714 | Birnbaum, H. K., and P. Sofronis | Hydrogen-enhanced localized plasticity—A mechanism for hydrogen-related fracture | July 1993 |
| 715 | Balachandar, S., and M. R. Malik | Inviscid instability of streamwise corner flow | July 1993 |
| 716 | Sofronis, P. | Linearized hydrogen elasticity | July 1993 |
| 717 | Nitzsche, V. R., and K. J. Hsia | Modelling of dislocation mobility controlled brittle-to-ductile transition | July 1993 |
| 718 | Hsia, K. J., and A. S. Argon | Experimental study of the mechanisms of brittle-to-ductile transition of cleavage fracture in silicon single crystals | July 1993 |
| 719 | Cherukuri, H. P., and T. G. Shawki | An energy-based localization theory: Part II—Effects of the diffusion, inertia and dissipation numbers | Aug. 1993 |
| 720 | Aref, H., and S. W. Jones | Chaotic motion of a solid through ideal fluid | Aug. 1993 |